# Quench echoes

**In spite of their seemingly random motion, atoms in computer-simulated glasses "remember" the time interval between a pair of freezings, simplifying certain many-body calculations.**

Sidney R. Nagel, Gary S. Grest and Aneesur Rahman

When we try to understand atomic motion in amorphous solids, we face a complicated problem in classical mechanics. What is the relationship between the motion of one atom and that of every other? Without a periodic crystal lattice to simplify the calculations, we must look for other properties that make things tractable. A phenomenon recently observed in computer models of many-body systems may give us such a simplification, at least in the calculation of a number of dynamical properties of glassy solids. This phenomenon, the "quench echo," appears as a brief but dramatic drop in the temperature of a theoretical solid sometime after it has experienced two abrupt quenches of its kinetic energy, as we will see later in detail.

Techniques of computer simulation have become increasingly important in physics, and there are now a variety of methods by which one can use them to investigate the complex behavior of many-body systems. Our intent here is not to review the merits and weaknesses of the various methods, but rather to focus on an example, the use of quench echoes in molecular dynamics, and see how this method applies to the important many-body problem of understanding the nature of the glassy state.

Computer simulations based on quench echoes are a powerful tool for studying the dynamics of solids. In this article we will describe the technique and look at the three main areas in which it has contributed so far: determining the density of states of normal modes in solids, determining the individual normal modes themselves and analyzing anharmonic behavior in solids. Normal modes are important because they are the elementary excitations of a solid from which we can calculate fundamental properties such as specific heat and thermal conductivity. While quench echoes have already shown themselves to be useful in isolating and studying these elementary excitations in glassy systems, they appear also to have applications in the study of such excitations in other complex $N$-body systems. As a consequence of their ability to isolate an elementary excitation, models using quench echoes have uncovered at high frequency a spatial localization of vibrational modes, and a sudden change of regime from localized to extended behavior with decreasing frequency. (See figure 1.) They have also made it possible to study, normal mode by normal mode, the frequency shift caused by a change in temperature or volume.

Sidney R. Nagel is associate professor of physics at the University of Chicago. Gary S. Grest is a staff physicist at Exxon's Corporate Research Science Laboratory, in Linden, New Jersey. Aneesur Rahman is a senior scientist in the materials science division of Argonne National Laboratory.

### The computer model

The many-body problem in classical mechanics is that of describing and understanding collective motion in complex systems of particles, and ultimately relating the structure and dynamics of such systems to the interparticle forces. We know from elementary mechanics that the two-body problem reduces to a simple quadrature. The three-body problem is quite another matter, and has a long and venerable history. When we change focus from a few-body problem to an $N$-body problem with $N$ about $10^{23}$, we enter the realm of statistical mechanics. Computers have added an extra dimension to the science of statistical mechanics through their ability to solve $N$-body problems for values of $N$ as high as 500 to several thousand.

The glassy state is an interesting $N$-body problem. We can think of a glass as a solid without crystalline order, as a homogeneous system with short-range but no long-range order. For such a system the usual methods of analysis are not very useful, and a numerical approach appears fruitful. In the following pages we will describe the quench echo phenomenon and see how it is used in molecular dynamics simulations to elucidate elementary dynamical excitations in glassy solids. It is a matter of opinion as to whether this sort of work should be considered experimental or theoretical in nature. We think it has elements of both.

In the method of molecular dynamics,[1] one integrates Newton's equations of motion numerically. Given the initial positions and initial velocities of all the particles, and the interparticle potential through which they interact, one calculates the new position and velocity for each particle at a time $\Delta t$ later (or earlier). For example, the constant-acceleration approximation gives for particle $i$,

$$r_i(t+\Delta t) = r_i(t) + v_i(t)\Delta t + \tfrac{1}{2}a_i(t)(\Delta t)^2$$
$$v_i(t+\Delta t) = v_i(t) + a_i(t)(\Delta t)$$

The acceleration is calculated from postulated forces of interaction between particle $i$ and all the other $(N-1)$ particles. After applying this algorithm to all the particles, one simply repeats the process. (In practice one uses a more efficient algorithm.) After many such cycles, the computer has calculated the trajectory for the system over some relatively long "macroscopic" time. In a simulation of atomic motion, this "macroscopic" time may be exceedingly short, on the order of $10^{-9}$ seconds.

The system on which we will concentrate in this article is a theoretical glass consisting of 500 particles in a box with periodic boundary conditions. That is, if a particle leaves one side of the box, it comes back in on the opposite face. Thus there are no surfaces in our computer model. The particles have hard-core radii $\sigma$ and interact with one another via the simplest realistic potential for solids, the


0031-9228 / 83 / 1000 24-09 / $01.00 

Lennard–Jones potential

$$V(r) = 4\epsilon\,[(\sigma/r)^{12} - (\sigma/r)^6]$$

Here $\epsilon$ is the depth of the potential, and $r$ is the separation between particles.

Because the system is classical, its instantaneous kinetic temperature is just proportional to the kinetic energy:

$$\tfrac{3}{2}kT = \tfrac{1}{2}m\langle v^2\rangle$$

Here the average is not over time, but over the $N$ particles, each of mass $m$. For argon, $\epsilon/k$ is 120 K, $\sigma$ is 3.4 Å and the unit of time $\tau$, given by $\sigma(m/\epsilon)^{1/2}$, is about $10^{-12}$ sec. The integration algorithm uses a time step $\Delta t$ of $0.01\tau$. It is convenient to use dimensionless parameters for temperature and density: $T^* = kT/\epsilon$, and $\rho^* = (N/V)\sigma^3$. The density $\rho^*$ for the experiments discussed in this article is 0.95. At this density the Lennard–Jones argon glass melts when $T^*$ is 0.80. At the triple point of the system $T^*$ is 0.70 and $\rho^*$ is 0.84. We form the system by rapidly cooling the liquid to a point where the particles do not diffuse over the time scale of the simulation.[2] For simplicity we call this frozen fluid a glass.

**The thermal quench.** The quench echo occurs when we lower the temperature in a particular way. We first quench the system at a time denoted by $t = 0$, that is, we stop all particles where they are and release them with zero velocity, thereby setting the kinetic energy and therefore the temperature instantaneously to zero. However, because each particle has potential energy, the particles immediately begin to move again, converting part of their potential energy back to kinetic energy. If the system were given sufficient time to return to equilibrium, its final temperature would be approximately half of its original value because the equipartition theorem is approximately valid at such low temperatures. The region on the left in figure 2a shows the temperature as a function of time during a period $t_1$ (45 time steps) after one such quench. To lower the temperature further, we quench the system again at time $t_1$. In addition to the expected lowering of temperature, this quench produces quite dramatic results. Instead of the temperature behaving simply as it did after the first quench, as one might expect, it displays the behavior seen on the right in figure 2a. An echo occurs at a time exactly $t_1$ after the second quench as the temperature suddenly drops and then quickly recovers its equilibrium value. There is no echo at time $2t_1$. This behavior does not depend on the value of $t_1$ as long as this time between quenches is longer than some critical time. Figure 2b shows how the depth of the echo depends on $1/t_1$; as the interval between the two quenches increases, the depth of the echo increases from zero to some maximum value and then decays at much longer times. As we shall see, the rate at which the echo decays depends on the starting temperature. For very low temperatures the echo should not decay at all, and no matter how long one waits to make the second quench, the echo should appear.

What happens if we quench the system a third time, at a time $t_2$ after the second quench? (Our convention throughout is that after each quench we start the clock over again.) Figure 2c shows the results. As we saw before, we find an echo at time $t_1$ after the third quench. But now we also find an echo at time $t_2$, and two new smaller echoes at times $|t_1 - t_2|$ and $t_1 + t_2$.

### Simple descriptions

We can explain the cause of these echoes with a very simple model.[3] Let us start by looking at what is happening in equilibrium before the first quench. The motion of the atoms is most easily analyzed in terms of the normal modes of vibration of the 500-particle solid. Each normal mode has a characteristic frequency. If the system

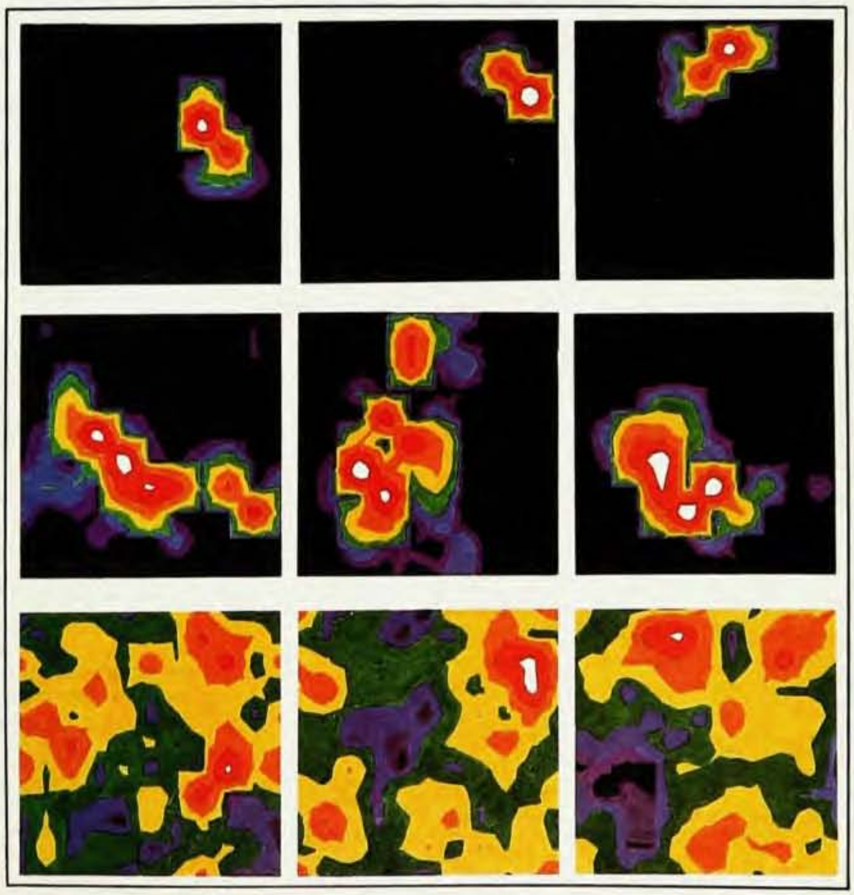

**Localization of normal modes** of vibration in a 500-particle glass. From left to right, the three frames in each row represent projections of the kinetic energy for a particular normal mode onto the $x$–$y$, $y$–$z$ and $z$–$x$ planes. Successive contours represent factor-of-two decreases in the kinetic energy. White represents the highest kinetic energy, red the next highest, and so on, down to black, which represents the least kinetic energy. The top row shows a highly localized normal mode in the glass. The normal mode in the middle row is of intermediate localization, and the normal mode in the bottom row is extended. From top to bottom, the normal modes have frequencies $\omega\tau$ of 28.9, 26.2 and 23.1. (Figure created by the authors with the help of Rudolph Banovich, University of Chicago.) Figure 1 is harmonic, the normal modes do not interact, or scatter from one another, and each normal mode contributes the same average amount to the total kinetic energy. Figure 3a shows this situation schematically. Each point represents a different mode of vibration of the 500 particles moving in an effective potential well represented by the parabolic solid line. For simplicity we have plotted all the modes in the same well, but we assume that each mode has a different frequency of oscillation. (Of course, in reality each mode moves in its own separate potential well.)

The quench at time zero forces all the modes to move vertically downward in the well because they lose all kinetic energy while their positions are left unchanged. At the end of this first quench all of the oscillators are pressed against the side of the well as shown in figure 3b. Subsequently, all the particles move toward the center of the well. Let us examine one small segment of the wall containing many modes with different frequencies. The same argument will hold for the rest of the wall. Those modes that have a low frequency move very slowly in this picture, and do not reach their classical turning points in time $t_1$. These are represented by the green point in figure 3c. Those modes that have a high frequency, shown in blue, move very quickly, and in time $t_1$ reach their classical turning points and come part of the way back. Finally there are those modes, shown in red, that have just the right frequency such that in time $t_1$ they just reach their classical turning points.

Now we quench the system for a second time. All the modes give up their kinetic energy and again drop vertically in the well. Thus the "green" modes and the "blue" modes lose a considerable amount of their total energy, whereas the "red" modes lose no energy at all, because they have no kinetic energy at the time of the quench. The kinetic energy, and therefore the temperature, becomes weighted by those modes that have the most total energy. After the second quench, those are the "red" oscillators. If we now watch what happens to the temperature of the system after the second quench, we see that at time $t_1$ the "red" oscillators have simply retraced their steps and are at rest at the side of the well, as figure 3d indicates. There they contribute nothing to the total temperature. The "blue" and "green" modes continue to move with the same frequencies as before, because in a harmonic well, the period of oscillation is independent of amplitude. Thus at time $t_1$ they do contribute a small amount to the kinetic energy, so the temperature does not go completely to zero. However, because it is the "red" oscillators that weight the temperature the most, the disappearance of their contribution causes a dip in the temperature, creating the observed echo.

This echo behavior does not depend on the solid being a glass. The essential requirement is that normal modes exist with a wide range of frequencies. This requirement is met in both glasses and crystals. The normal modes exist with frequencies from zero—the sound modes—up to the highest allowed frequency—usually near the Debye frequency $\omega_D$. It is the fact that there is a highest frequency normal mode in the solid that accounts for the absence of an echo when the time between quenches is too small.

**Metasimulation and lab demo.** We can put this description into much more concrete terms by simply writing out the temperature as a function of time for a harmonic system both before and after each quench. The box on page 28 shows the relevant equations. By examining these equations we can understand in detail the behavior described so far. In particular, we see from equations 2 and 3 why there is no echo at time $2t_1$ after a series of two quenches, and from equation 4 why there are echoes at times $|t_1 - t_2|$ and $(t_1 + t_2)$ after a series of three quenches.

To show that this is indeed the correct explanation for the echo phenomenon, we can use equation 2 and assume a density of states that is similar to what we have in our Lennard-Jones glass. Thus, in effect, we are doing a simulation of our simulation! The deep echo in this "metasimulation" (figure 4) is very similar to that seen in the computer "data" (figure 2a). We can also use this method to calculate the depth of the echo as a function

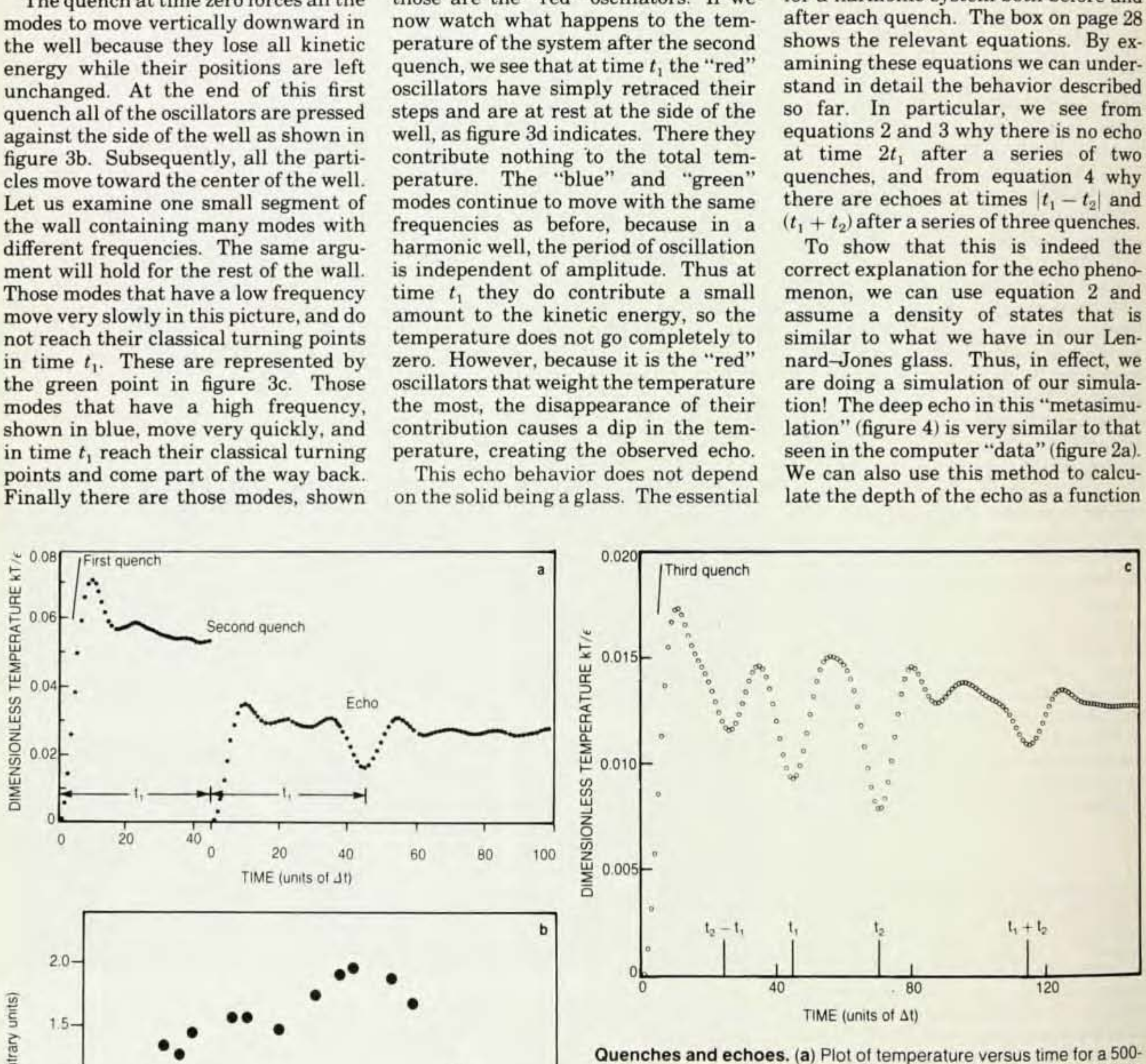


**Quenches and echoes.** (**a**) Plot of temperature versus time for a 500-particle system quenched twice. The interval $t_1$ between quenches is $45\Delta t$, where the time step $\Delta t$ is about $10^{-14}$ sec. Convention is to initialize the clock after each quench. (**b**) Depth of the echo versus the reciprocal of the time between quenches. (**c**) Plot of temperature versus time after the system is quenched twice as in **a**, and then a third time. The interval $t_2$ between the second and third quenches is $70\,\Delta t$. The times for four echoes are indicated. Figure 2

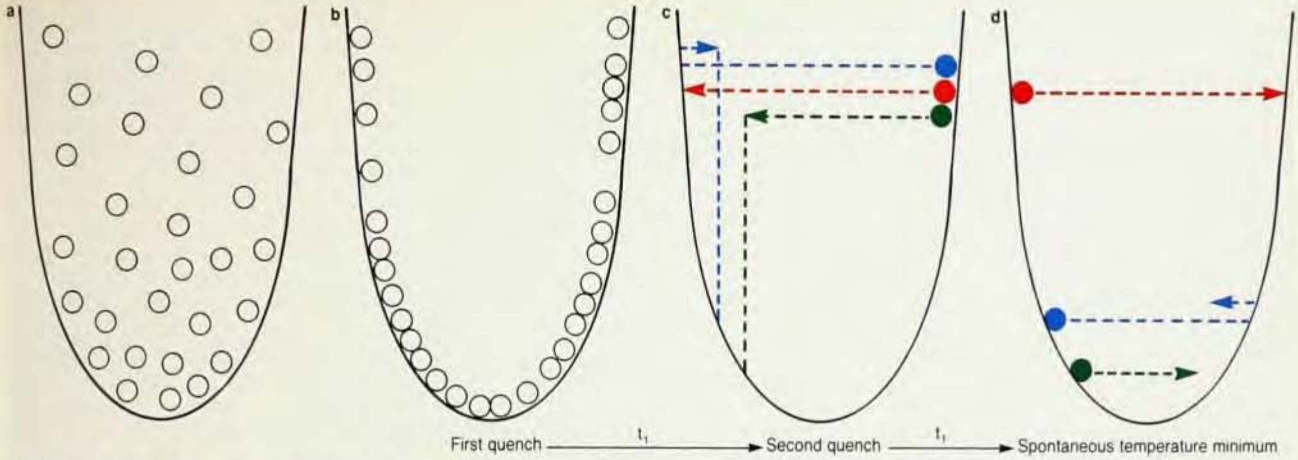


**Model** to explain quench echo phenomena. Each point represents a different mode of vibration of 500 particles that make up a solid. Each mode has its own frequency of oscillation; for simplicity, all modes appear here in the same effective potential well, represented by a parabola. The second quench selects modes with period $t_1$ (red). Modes of other frequencies (blue and green) lose energy. Figure 3

of the time $t_1$ between quenches. The result does show structure similar to that in figure 2b, except for one characteristic. As the time between quenches increases, the depth of echo does not decay but remains constant. We will get back to this point later when we discuss the effect of anharmonicity on the echo. We may also ask what contributes to the width of the echo. The width is simply determined by the highest-frequency normal mode. If we define $\delta t$ as $|t - t_1|$, then we can see from equation 3 that when $\delta t > \pi/\omega_D$ the echo starts to disappear as some modes no longer contribute to it. Studies of samples of various sizes show that the width does not depend on the number of particles in the sample.

One can perform a very simple experiment in an undergraduate mechanics laboratory to show the existence of the echo and demonstrate that it does not depend on a Maxwell's Demon for its production. With the suggestions and assistance of David Hwang, John Carini and Shobo Bhattacharya, we have had some success with this experiment. We model a one-dimensional solid by placing on an air-track a row of masses connected by springs, as shown in figure 5. When the air is turned on, the masses move along the track without friction. However, when the air is turned off, the masses immediately stop moving because of friction with the track. Turning off the air thus corresponds to a quench, because it removes the kinetic energy while leaving the positions of the masses unchanged. (The masses stop moving in a small fraction of a period of oscillation.) The experiment is as follows: We start the masses moving randomly, and then turn off the air. This is the first quench. We then turn on the air again and wait a time $t_1$. Turning off the air again corresponds to the second quench. When we turn on the air again we watch the masses very carefully, and at a time $t_1$ after the last quench we see that they all slow down for a moment and then speed up again. The best way to see this echo is to make a movie and show it in slow motion. Of course, one must be sure to watch for a dip in the total kinetic energy of the system and not just the slowing of a few masses.

It is interesting to note that there are also "heat echoes," dramatic increases in temperature after two abrupt heat pulses. However, because a heat pulse adds energy to all modes, these echoes are more difficult to observe. If we start at very low temperatures ($T^* \leq 10^{-6}$) and suddenly increase the velocity of each atom by a factor of $10^3$ at two successive times $t_1$ steps apart, then the temperature $T^*$ shows a broad maximum at a time $t_1$ following the second pulse. However, to observe this heat echo we have to apply large heat pulses and start at very low temperatures, so as not to vaporize the system. Because of these limitations, heat echoes turn out to be less useful than quench echoes in studying the properties of the system.

The quench echo can be developed into a powerful technique to study the dynamic behavior of solids using computer simulations. This has occurred in three main areas so far.

**Density of states.** The first of these is the determination of the density of states $D(\omega)$ of a solid's normal modes. There are two different ways of doing this. Clearly the depth of the echo appearing at time $t_1$ should be related to the number of modes with frequency $\omega = \pi/t_1$. If we quench the system many times with the same interval $t_1$ between quenches, the subsequent behavior of the temperature will tell us how many modes have that frequency. This is a long, involved process. It turns out that there are better ways of determining the density of states, one of which also uses the quenching process.[4] If we look at figure 2a—the time dependence of the temperature after one quench—we see that the curve has some structure that we have neglected up to now. This structure contains information about the density of states. From equation 1 in the box, we see that

$$T^*(t) = \int_0^\infty D(\omega)A^2(\omega)\sin^2\omega t\, d\omega$$

We can solve this for the density of states by taking the Fourier transform of the temperature $T^*(t)$. Thus, in the case of the harmonic system, the function $T^*(t)$ contains the same information as the velocity autocorrelation function.

**Anharmonic behavior.** The second use to which one may put these echo techniques is in analyzing a solid's anharmonic behavior. There are at least three different ways of doing this.

▶ As we saw in figure 2b, as the time $t_1$ between quenches become large, the depth of the echo decays. However, as we mentioned earlier, if we assume a harmonic system, choose an appropriate density of states and use equation 3, we find that the depth of echo does not decay, but approaches a constant at large times. We observe a decay of the echo because our glass is not perfectly harmonic but has considerable anharmonicity in its motion even at low temperatures. Looking at equation 3, we see that because the sum is over many different frequencies, all the terms but two average to zero when the times $t$ and $t_1$ are large. The terms that survive leave us with the following expression for the temperature at long times

$$T^*(t) \simeq \Sigma_i (A_i^2/4)[1 - \tfrac{1}{2}\cos\omega_i(t - t_1)]$$

The depth of the echo should therefore approach a constant value in the harmonic system because when $t$ is $t_1$, the temperature is one-half of its average value, the average value of the last term being zero. By observing the dependence of the echo depth on time, one can determine the strength of the anharmonic forces that give rise to interactions between normal modes, making them lose phase coherence with respect to one another.

▶ Another way to analyze anharmonic behavior is to monitor the temperature after three quenches.[5] In a harmonic system, if one quenches at time 0, at time $t_1$ after that, and at time $t_2$ after that, the subsequent behavior of the system should be identical to that of a system quenched in inverted order, that is, at time 0, at time $t_2$ after that, and at time $t_1$ after that. We can perform both computer experiments and compare the results. If we start with the glass at very low temperature, say $T^* = 0.001$, then we indeed find identical behavior in the two sequences of quenches. However, when we raise the temperature, we quickly begin to see significant differences between the two temperature curves. These differences show how the anharmonicity in the motion increases with temperature. The sequence of frames in figure 6 shows the appearance of these differences in a Lennard-Jones glass as the initial temperature increases. Interestingly, at the highest temperature the system is actually a liquid and it is still possible to see a weak echo.

▶ A third way of detecting anharmonic behavior is to measure the decay of what is called the "stimulated" echo. This echo is created by quenching the system at time 0 and again at time $t_1$. We then wait a variable length of time $t_2$ and quench once again. The stimulated echo appears at a time $t_1$ after this last quench. The echo at time $t_1$ in figure 2c is thus a simulated echo. We can measure the depth of this echo as a function of the time we waited, $t_2$. The echo decays with this waiting time according to the strength of the anharmonic interaction between modes. In a rubidium glass, the echo decays much more slowly with waiting time than it does in a Lennard-Jones glass, indicating that a harmonic approximation such as the one in the box below gives a more accurate description of the former than it does of the latter. This is consistent with the experimental fact[6] that Lennard-Jones liquids, such as liquid argon, do not support propagating sound modes out to large wavevectors, whereas liquid rubidium does.

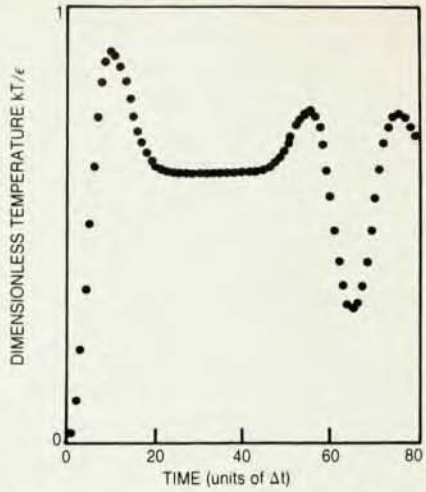


**Metasimulation.** This plot of temperature versus time is the result of using a simple equation (equation 2 in the box below) and a realistic density of states to simulate the quench echo phenomenon, which itself is seen in simulations of solids. The interval between quenches is $65\Delta t$. Figure 4

**Individual normal modes.** The final use that we will describe here for quench echos is to obtain the individual normal modes themselves. The process[7] is very simple. If we quench the system at time 0 and again at time $t_1$, those modes having frequency $\omega = n\pi/t_1$, where $n$ is an integer, survive best. If we quench the temperature again at a time $t_1$ after the last quench, the predominance of those same frequencies gets even more pronounced. If we now repeat the quenches many times, each separated by the same interval $t_1$ (or some integral multiple of it) the system eventually begins to have only one frequency or its harmonics in its motion; it is quite easy to quench out all of the harmonics. Neglecting degeneracies, this leaves only one normal mode oscillating in the sample. This method of repeated quenches becomes useful when we are dealing with a very large system with long-range interactions. Normally, to obtain the normal modes one would simply diagonalize the dynamical matrix.[8] In practice, however, this becomes very difficult for large systems because the size of the matrix one can diagonalize is severely limited by computer storage capacity. Thus the quench-echo technique for finding normal modes—the eigenfunctions of the dynamical matrix—becomes very useful for large samples. By simply varying the time $t_1$ between quenches one selects normal modes with different frequencies, a process that requires less computer storage than does matrix diagonalization.

Let us look now in detail at the use of quench echoes in determining the normal-mode structure in a Lennard-Jones glass. There are two problems we would like to discuss. The first is the question of the spatial extent of the modes. In the same sense that electrons can be localized in a disordered medium, phonons can also have a critical frequency dividing localized from extended states. The question of localized states has played a fundamental role in amorphous semiconductors, where the character of the electronic

## Harmonic approximation

Before the first quench:

$T^*(t) = \sum_i A_i^{*2} \sin^2(\omega_i t + \phi_i)$, where $A_i^*$ and $\phi_i$ are random.

After the first quench but before the second quench:

$$T^*(t) = \sum_i A_i^2 \sin^2(\omega_i t) \qquad (1)$$

After the second quench but before the third quench:

$$T^*(t) = \sum_i A_i^2 \cos^2\omega_i t_1 \sin^2\omega_i t \qquad (2)$$

$$= \sum_i (A_i^2/4)[1 + \cos 2\omega_i t_1 - \cos 2\omega_i t - \tfrac{1}{2}\cos 2\omega_i (t + t_1) - \tfrac{1}{2}\cos 2\omega_i (t - t_1)] \qquad (3)$$

After the third quench:

$$T^*(t) = \sum_i A_i^2 \cos^2\omega_i t_1 \cos^2\omega_i t_2 \sin^2\omega_i t$$

$$= \sum_i (A_i^2/2)[\cos^2\omega_i t_1 + \cos^2\omega_i t_2 + \tfrac{1}{2}\cos^2\omega_i (t_1 + t_2) + \tfrac{1}{2}\cos^2\omega_i (t_1 - t_2) - 1] \sin^2\omega_i t \qquad (4)$$

After many $(N + 1)$ equally spaced quenches:

$$T^*(t) = \sum_i A_i^2 \cos^{2N}\omega_i t_1 \sin^2\omega_i t$$

**Masses and springs.** One can observe quench echoes in a simple airtrack experiment. Quenches are carried out by turning off the air abruptly, which stops the masses within a small fraction of a period. This deprives them of their kinetic energy but not their potential energy. Some time after a pair of such quenches there is a brief spontaneous drop in the kinetic energy. The waiting time for this "echo" is equal to the time between the two quenches. (Photograph courtesy of Daedalon Corporation, Salem, Massachusetts.) Figure 5

state determines the transport properties. (See Jan Tauc's article on amorphous semiconductors, PHYSICS TODAY, October 1976, page 23.) We would like to study the character of the phonon states. The second problem is to determine the dispersion curve for the normal modes over their entire frequency range.

### Localization of modes

We would expect the highest-frequency modes to be the most localized, just as in the case of electrons, where it is the band tails that have localized states and the band center that has extended states. In the case of phonons, it is only the high-frequency modes that become localized; modes near $\omega = 0$ correspond to sound waves, which are the very last modes to be localized. We again expect a localization threshold, marking the boundary between extended and localized states.

The phonons in a glass are a particularly revealing system to study, not only because we can analyze the frequency dependence of localization in the same way that we analyze the energy dependence of localization with electrons, but because we can also add interactions between normal modes and study what happens in a strongly interacting system. We can observe the effect of interactions by simply increasing a mode's amplitude of oscillation. At low amplitudes the mode is in a harmonic regime and does not interact. At high amplitudes it does interact with other modes because of the anharmonic terms in the potential. In this case we are actually studying an interacting many-body system. This effect of amplitude variations gives us an extra degree of freedom in phonon simulations that we do not normally find in simulations of electronic systems.

By asking the computer the amplitude and polarization of each particle in each normal mode, we find out which modes are localized and which are extended.[7] There are two particularly interesting quantities that we can calculate to help distinguish these two behaviors. The first is the inverse participation ratio, $\langle v^4\rangle/\langle v^2\rangle^2$. When the oscillations extend throughout the system, this quantity has a value of order unity, whereas when the oscillations are localized, it has a larger value and is proportional to the number of particles participating in the mode. The other quantity of interest is the kinetic energy correlation function:

$$h(r) = \sum_{i,j} v_i^2 v_j^2\, \delta(r - r_{ij}) / \sum_{i,j} \delta(r - r_{ij})$$

Here $r_{ij}$ is the distance between particles $i$ and $j$. For localized modes, if two particles are far apart, then at most only one of them can participate strongly in the mode and thus have a large kinetic energy. Hence the product $v_i{}^2 v_j{}^2$ is small for large $r$ and the correlation function $h(r)$ falls off rapidly at large $r$. In an extended state, on the other hand, two particles separated by a large distance can both contribute to the motion. Thus the correlation $h(r)$ does not decay for extended modes.

Figure 7a shows the behavior of the correlation function for two modes, one highly localized and one extended. The function $h(r)$ for the extended mode does not decay over the extent of our sample, whereas for the localized mode it decays by three orders of magnitude in only four interatomic distances. Figure 7b shows the behavior of the inverse participation ratio as a function of frequency. The slope of the kinetic energy correlation function shows a similar frequency dependence. Figure 7c shows the density of states $D(\omega)$ for this system. At high $\omega\tau$, that is, for $\omega\tau$ above 24.5, the modes are all clearly localized. Below that frequency they are all extended. This shows that there is a threshold between the localized and extended modes.

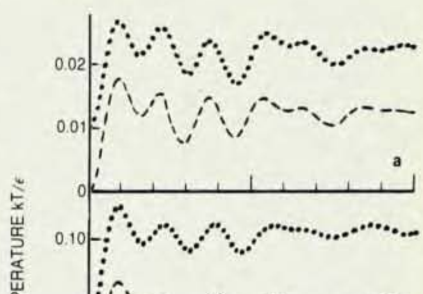


**Lennard–Jones system's** response to three quenches. These temperature-versus-time curves begin after three quenches separated by times $t_1$ and $t_2$. For the dotted curves, $t_1$ is $30\Delta t$ and $t_2$ is $45\Delta t$. For the dashed curves, these times are interchanged. The dotted curve is displaced vertically to make it easier to see. The initial temperatures $kT/\epsilon$ are 0.11 in **a**, 0.46 in **b** and 1.2 in **c**. Figure 6

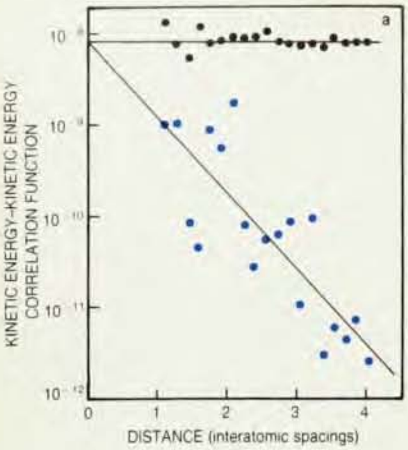


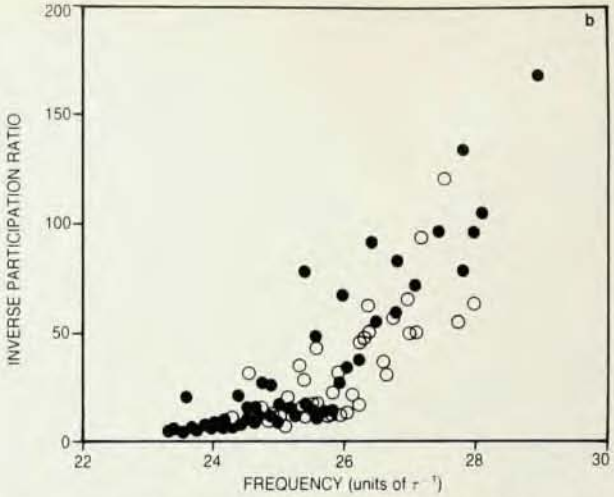


**Correlation,** participation and density of states. **(a)** Plot of the kinetic energy–kinetic energy correlation as a function of distance, for an extended mode with $\omega t = 21.3$ (black) and for a localized mode with $\omega t = 28.9$ (color). **(b)** Inverse participation ratios as a function of frequency for two 500-particle glasses (open and closed circles) with a density $\rho^*$ of 0.95. **(c)** The density of states for the system in **b**. Figure 7

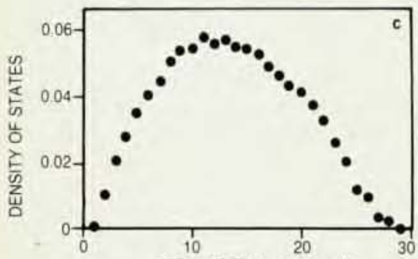


**Experiment.** An obvious question is: How can one determine experimentally whether a mode is localized or extended? One might consider looking at the "dynamic structure factor" derived from inelastic neutron scattering experiments. However, as we shall see when we discuss the dynamic structure factor for all the modes in a glass, this quantity is completely insensitive to a mode's degree of extension.

Another method one might use to look for the difference between extended and localized modes is to study their anharmonic behavior. One common way[9] of characterizing the anharmonicity of a mode is to measure its "Grüneisen parameter." This parameter, too, turns out not to be a good measure of localization. Let us nevertheless look at how it works, because later it will be instructive to see exactly why it is not a good measure of localization. The Grüneisen parameter $\gamma_i$ is defined as $d(\ln\omega_i)/d(\ln V)$, where $\omega_i$ is the frequency of the $i$th normal mode, and $V$ is the volume of the system. For a perfectly harmonic system, the frequency of a mode is independent of the volume, so the Grüneisen parameter is zero. We can measure a mode's Grüneisen parameter in our simulations by changing the number density of particles and noting the resulting change in the mode's frequency of oscillation in the sample. For reasons we will see, calculations of the Grüneisen parameter for many modes, both localized and extended, show no change as one moves across the localization threshold.

One can also measure the anharmonicity in a mode by observing how the mode's frequency shifts with the amplitude of vibration. In a harmonic mode it does not shift at all. We can measure this frequency shift in our simulation as well. The result is that for frequencies below the localization threshold, $d(\omega\tau)/dT^*$ is very small, where $T^*$ is now the temperature, or amplitude, of the particular mode we are studying. Above the threshold, however, this measure of anharmonicity grows rapidly with increasing frequency. There seems to be a slight contradiction here. Whereas the anharmonicity as measured by the Grüneisen parameter does not show a difference between localized and extended modes, the anharmonicity as measured by $d(\omega\tau)/dT^*$ does. We can make a very simple model that indicates why this difference might appear. In the case of $d(\omega\tau)/dT^*$, we can argue as follows. If two modes, one localized and one extended, are close in frequency and have the same amount of kinetic energy (which is to be expected because $\hbar\omega$ would be almost the same for both), the localized mode will have much more kinetic energy in each of its atoms. Because these atoms will then have a much larger amplitude of vibration, they will explore the anharmonic parts of the potential to a greater extent than will the atoms in the extended mode. Thus, the frequency of a localized mode will be much more sensitive to the mode's total energy than will the frequency of an extended mode. This argument does not apply to the case of the Grüneisen parameter.

As a final observation on the difference between localized and extended normal modes in glass, let us see how the positions of the atoms change with temperature. When a mode is excited with a low amplitude of vibration, each atom oscillates about some equilibrium position. As the level of excitation increases, the atoms not only move with greater amplitude about their central positions, but the central positions themselves move. The root mean square drift is proportional to the temperature. This motion of atoms is often not as significant in simple crystals where the high degree of symmetry confines the atoms to vibrate about fixed symmetry positions. A glass has no such symmetry restrictions, so the drift is present in all the modes. As in the case of the frequency shift with amplitude, the effect is much larger for localized than for extended modes, and this is another physical manifestation of the difference between extended and localized states.

## Dispersion curves

The dynamic structure factor $S(k,\omega)$ for the vibrational modes in a glass is the space and time Fourier transform of the correlation function that describes the spatial and temporal fluctuations of density in the system. We can calculate this factor and use it to analyze longitudinal excitations, which one can measure through inelastic neutron scattering; we can do an analogous calculation for the transverse excitations.[10–12] The generalization of the structure factor to transverse modes, $C_\perp(k,\omega)$, while not directly measurable, has been valuable in the study of liquids.

Figure 8b shows[11] the function $f_\parallel(k,\omega)$, for eight normal modes of a 250-particle glass, where $f_\parallel(k,\omega)$ is the one-phonon part of the dynamic-structure factor $S(k,\omega)$ to within some smoothly varying factors. For a mode of frequency $\omega$, this function is given by

$$f_\parallel(\mathbf{k},\omega) = \left\langle \left| \sum_i \hat{\mathbf{k}}\cdot\mathbf{P}_i^{\omega} e^{i\mathbf{k}\cdot\mathbf{r}_i} \right|^2 \right\rangle$$

Here $\mathbf{P}_i^{\omega}$, the polarization vector, is the maximum displacement of the $i$th atom vibrating in the mode, and $\mathbf{r}_i$ is the position of the atom. The brackets indicate that the quantity is averaged over all wavevectors $\mathbf{k}$ of a given magnitude.

We see that there are well-defined

peaks in the one-phonon part of the dynamic-structure factor for both very-low- and very-high-frequency modes. For the modes with lowest nonzero frequency, which correspond to sound waves, there are two regions of interest in the wavevector $k$. When $k$ is small, as with the mode giving rise to the plot in the first frame of figure 8b, $f_\parallel(k,\omega)$ decreases monotonically with increasing wavenumber, and we do not see the low-$k$ part of the peak that corresponds to sound waves. However, for the same mode ($\omega\tau = 1.3$) there is also a well-defined broad peak near a wavevector $k$ of magnitude $7\sigma^{-1}$. This value of the wavevector corresponds to the first peak in the static structure factor. In a crystal, for wavevector k near the first reciprocal lattice vector, one would get a peak at low frequency to which this peak at $k\sigma = 7$ corresponds. At higher frequency, when $\omega\tau$ is near 10, the first peak—the one corresponding to sound waves—appears fully and is quite sharp. For yet higher frequency, this peak in $f_\parallel(k,\omega)$ becomes quite broad in wavevector. For this reason, large wavevectors are not considered to be "good" eigenvectors in a glass. This can be seen when $\omega\tau$ is about 14, and the two peaks are both small and ill-defined. The surprising fact is that as the frequency increases further, the peaks do not become broader in $k$, but become better defined and quite clear for the highest-frequency modes, some of which are highly localized in space. It is very remarkable that there is so much structure to be seen in $S(k,\omega)$ for a glass even in the region away from wavevector zero.

Studies[10,11] of transverse excitations in glasses show that at low frequencies the transverse dynamic structure factor $C_\perp(k,\omega)$ has a pronounced structure at small wavevectors. As the frequency increases, the structure broadens, and for values of $\omega\tau$ near 17, it is almost completely gone. However, at higher frequencies, $C_\perp(k,\omega)$ again begins to peak more clearly, even though these are highly localized states. There is one very clear difference between the behavior of transverse and longitudinal modes. For the longitudinal excitations, there are always multiple peaks for each normal mode, although as we saw, the peaks become indistinct when $\omega\tau$ is near 12. However, the transverse excitations show only one clear peak for most modes. Only at high frequencies, when $\omega\tau$ exceeds 23, does a second, very broad peak begin to emerge above the background at higher wavevector.

From the type of data shown in figure 8b, one can construct a dispersion curve for the normal modes. Figure 8a shows the result of a plot of the frequency against the wavevectors for which the function $f_\parallel(k,\omega)$ has its first two maximum values. There is a re-

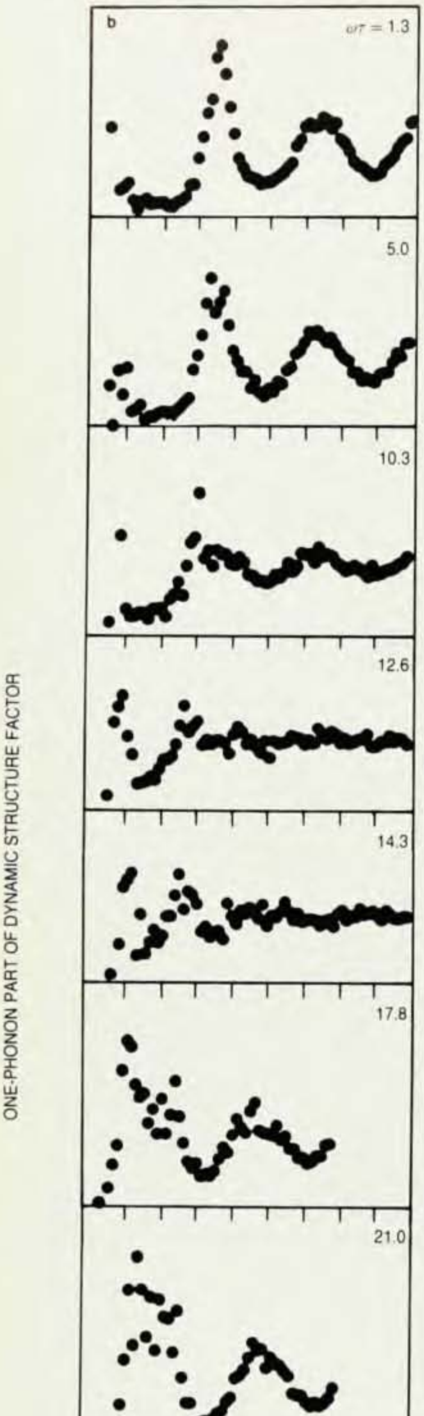


markably deep minimum in the dispersion curve near the point where $k\sigma$ is 7, which is the wavevector for which the static structure factor has its first sharp maximum. Early calculations[13] for one-dimensional models indicated the existence of such a structure. A recent calculation[14] using an average dynamical matrix has reproduced these results qualitatively.

The results for the excitations in a glass bear a striking resemblance to what one finds for a polycrystalline material. In particular, the dispersion curve for longitudinal excitations shows the same overall structure, with a minimum occurring near the peak in the static-structure factor for a glass, or near the first reciprocal lattice vector for a polycrystal. The shapes of the curves for $f_{\parallel}(k,\omega)$ also show similarities. The longitudinal sound peak gets broader with increasing frequency in both the glass and the polycrystal. In the region where $\omega\tau$ is near 12, the valley between the peaks has begun to fill up in the polycrystalline sample, corresponding to the lack of structure seen in the glass in the same frequency range. In the transverse modes, similarities still exist between the glass and the polycrystal, but they are less dramatic. The velocity of transverse sound in the glass is approximately 20% smaller than in the crystal. Most unexpected is that in the polycrystal the transverse dispersion curve does show signs of a zone boundary and of a repeated zone scheme, whereas in the glass there is no sign of the transverse modes having a second peak with intensity significantly above the background near a wavevector of magnitude $7\sigma^{-1}$.

J. Hafner of the Institute for Theoretical Physics in Vienna, Austria, uses[15] a simple model to argue that the structure that appears in $f_{\parallel}(k,\omega)$ near the point where $k\sigma = 7$ for low-frequency excitations is due to a process

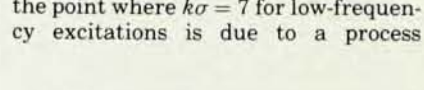


**Dispersion and dynamic structure. (a)** The dispersion curve for longitudinal excitations. **(b)** The one-phonon part of the dynamic structure factor is plotted here as a function of momentum, for eight normal modes of a 250-particle glass. Figure 8

analogous to what is called Umklapp scattering[9] in crystalline solids. The first sharp maximum in the static structure factor of the glass acts like a smeared-out reciprocal lattice vector in a crystal. He suggests that this "diffuse Umklapp scattering" of low-wavevector transverse excitations contributes nearly all of the peak's intensity at high wavevectors such as $7\sigma^{-1}$. Models using quench echoes verify this prediction.

Computer simulations have been able to provide much insight into the static and dynamic properties of glasses. Quench echoes represent one more tool at our disposal for studying the behavior of this important many-body problem. Our final objective, of course, is to understand the nature of all the elementary excitations in an amorphous system. The size of current computers limits us to relatively small samples. With computers continuing to grow in speed and storage capacity, we will soon be able to study the truly low-frequency excitations in glasses.

### References


1. For a general review of molecular dynamics simulations, see R. W. Hockney, J. W. Eastwood, *Computer Simulations Using Particles*, McGraw-Hill, New York (1981).
2. A. Rahman, M. J. Mandell, J. P. McTague, J. Chem. Phys. **64**, 1564 (1976); C. S. Hsu, A. Rahman, J. Chem. Phys. **71**, 4974 (1979).
3. G. S. Grest, S. R. Nagel, A. Rahman, Solid State Commun. **36**, 875 (1980).
4. G. S. Grest, S. R. Nagel, A. Rahman, T. A. Witten Jr., J. Chem. Phys. **74**, 3532 (1981).
5. G. S. Grest, S. R. Nagel, A. Rahman, J. de Physique (Paris) **41**, C8-293 (1980).
6. D. Levesque, L. Verlet, J. Kurkijarvi, Phys. Rev. A **7**, 1690 (1973); A. Rahman, Phys. Rev. A **9**, 1667 (1974); H. Bell, H. Moeller-Wenghoffer, A. Kollmar, R. Stockmeyer, T. Springer, H. Stiller, Phys. Rev. A **11**, 316 (1975).
7. S. R. Nagel, A. Rahman, G. S. Grest, Phys. Rev. Lett. **47**, 1665 (1981).
8. The pioneering work in this area was by R. J. Bell and P. Dean; for a review, see R. J. Bell in *Methods in Computational Physics*, G. Gilat, ed., Academic, New York (1976), Vol. 15, page 215.
9. N. W. Ashcroft, N. D. Mermin, *Solid State Physics*, Holt, Rinehart and Winston, New York (1976).
10. J. Hafner in *Glassy Metals I*, H. -J. Güntherodt, H. Beck, eds., Springer-Verlag, Berlin (1981).
11. G. S. Grest, S. R. Nagel, A. Rahman, Phys. Rev. Lett. **49**, 1271 (1982).
12. J. -B. Suck, H. Rudin, H. -J. Güntherodt, H. Beck, Phys. Rev. Lett. **50**, 49 (1983); J. Phys. C **14**, 2305 (1981).
13. S. Takeno, M. Goda, Progress in Theoretical Physics **47**, 790 (1972).
14. L. M. Schwartz, Phys. Rev. Lett. **50**, 140 (1983).
15. J. Hafner, J. Phys. C **14**, L287 (1981).